# Chapter 7
# On the Physical Vulnerability of Buildings Exposed to Landslide Hazards in the Lisbon Metropolitan Area


**Ana Cardoso, Susana Pereira, Tiago Miguel Ferreira, José Luís Zêzere, Raquel Melo, Teresa Vaz, Sérgio Cruz Oliveira, Ricardo A. C. Garcia, Pedro Pinto Santos, and Eusébio Reis**

**Abstract** This study assesses the physical vulnerability of buildings (PVB) in the Lisbon Metropolitan Area (LMA) exposed to landslides triggered by both rainfall and earthquakes. Firstly, a statistical model (Information Value), validated with a ROC curve, was adopted to assess susceptibility to landslides caused by rainfall. Secondly, an Analytic Hierarchy Process was adopted to assess the susceptibility to landslides caused by earthquakes. In this case, the model was validated with an inventory of historical landslides in the LMA. The vulnerability assessment included all

A. Cardoso · S. Pereira · J. L. Zêzere · T. Vaz · S. C. Oliveira · R. A. C. Garcia · P. P. Santos · E. Reis
Centre for Geographical Studies, Institute of Geography and Spatial Planning (IGOT), LA TERRA, University of Lisbon, Lisbon, Portugal
e-mail: amcardoso@campus.ul.pt

J. L. Zêzere
e-mail: zezere@igot.ulisboa.pt

T. Vaz
e-mail: tvaz@campus.ul.pt

S. C. Oliveira
e-mail: cruzdeoliveira@campus.ul.pt

R. A. C. Garcia
e-mail: rgarcia@igot.ulisboa.pt

P. P. Santos
e-mail: pmpsantos@campus.ul.pt

E. Reis
e-mail: eusebioreis@campus.ul.pt

S. Pereira (✉)
Faculty of Arts and Humanities, Geography Department, University of Porto, Porto, Portugal
e-mail: sspereira@letras.up.pt

R. Melo
Institute of Earth Sciences, School of Science and Technology, University of Évora, Évora, Portugal
e-mail: raquel.melo@uevora.pt



T. M. Ferreira (ed.), *Multi-risk Interactions Towards Resilient and Sustainable Cities*, Advances in Sustainability Science and Technology,
https://doi.org/10.1007/978-981-99-0745-8_7

residential buildings surveyed in the 2011 Census, considering a set of vulnerability parameters, namely: the presence of reinforced structure, number of floors, conservation status, and need for repairs in the structure and finishes. These parameters, and their respective weights, were based on expert opinion and literature. Through this analysis, it was possible to identify meaningful regional interactions between the earthquake and rainfall-triggered landslides, leading to complex damage scenarios for residential buildings. It was also possible to identify risk hotspots and potential risk adaptation and mitigation measures.

**Keywords** Landslides · Physical vulnerability · Rainfall-triggered landslides · Earthquake-triggered landslides · Lisbon Metropolitan Area

## 1 Introduction

Landslides are responsible for major fatalities, generating large human, social and economic losses. Landslides are complex processes with multiple causes, which can occur simultaneously; the final cause is nothing more than a triggering mechanism, which corresponds to the final push of a mass that was already on the verge of rupture. Rainfall and seismic activity are the main triggers of landslides, having already been characterized at the regional scale for some areas in Portugal, namely, the Lisbon region, with studies concerning the susceptibility of rainfall-triggered landslides (RTL) [36, 38]. Works concerning earthquake-triggered landslides (ETL) in Portugal are scarcer since the landslides triggered by this phenomenon are less frequent and older [30].

It is important to consider the context of this work in the current and future framework of the problematic climate situation. Araújo et al. [3], through RCP (Representative Concentration Pathways) emission scenarios: RCP 4.5 and RCP 8.5, which consider the existence of an increase in radiative forcing by 4.5, and 8.5 W/m$^2$ by the year 2100, respectively, studied and evaluated the impact of extreme precipitation (defined as the amount of precipitation needed to trigger a landslide, rainfall triggering threshold—RTT) on future landslides. This analysis was performed for two locations: Sobral de Monte Agraço (SMA), in the Grande da Pipa river basin, located in the Lisbon district; and Santa Marta de Penaguião (SMP), belonging to the Douro river basin, in the north of the country. For both locations, four thresholds were determined relative to the number of consecutive days with accumulated precipitation: 1D (one day), 10D (10 days), 30D (30 days), and 60D (60 days). The forecast of the RCP4.5 scenario, concerning days with accumulated precipitation mentioned above, shows, in all cases mentioned, an increase in extreme precipitation, between 3 and 10%. In the opposite direction, the forecasts of the amount of future precipitation,

T. M. Ferreira
School of Engineering, College of Arts, Technology and Environment (CATE), University of the West of England (UWE Bristol), Bristol, UK
e-mail: Tiago.Ferreira@uwe.ac.uk

for the RCP8.5 scenario, indicate a decrease in extreme precipitation for 10, 30, and 60 days of accumulated precipitation, for SMA. This suggests that for the RCP4.5 scenario (the most conservative), more extreme precipitation events will occur, with the RTT required for triggering slope movements. For the RCP8.5 scenario, more one-day extreme precipitation events are predicted to occur, isolated episodes with a large concentration of precipitation, with the RTT, required for triggering slope movements, which may lead to an increase in the number of translational surface landslides (associated with intense precipitation events with short duration periods); however, in SMA, the projection of precipitation for 10, 30, and 60 days, has a negative relative difference, which translates to a decrease in the average annual precipitation [19, 24] and a decrease in the occurrence of deeper slope movements (associated with longer precipitation events) [3].

There are several works with records of damage caused by landslides, the most frequent referring to damage caused to population, roads, and buildings, such as the landslides triggered by the seismic event of 1512 (magnitude of 6.3 on the Richter scale) in Lisbon, which destroyed about 200 houses and caused the death of 2,000 people, with a rupture surface between 5 and 7 m [30, 31], and the seismic event of 1597 (magnitude of 5.7 on the Richter scale), which destroyed three streets and 110 houses, with a rupture surface between 15 and 20 m [29, 31].

RTL also causes damage to the population and to different types of structures, buildings, and roads. The DISASTER database identified, in the LMA, for the period from 2006 to 2020, 5 occurrences of landslides movements involving human damage: on October 24, 2006, a rockfall in Almada caused one fatality and, on March 15, 2018, in Colares (Sintra), another rockfall caused one fatality and four injuries. In 2010, there were two mass movements that affected ten buildings, leaving four people homeless [37]. Alves and Oliveira [2] identified 356 landslides that caused damage to roads in the Rio Grande da Pipa basin through the interpretation of aerial photographs and orthophoto maps.

The physical vulnerability of buildings (PVB) refers to the predisposition of the building to suffer damage derived from the occurrence of a potentially destructive natural phenomenon [27] and ranges on a scale from 0 (no damage) to 1 (total damage). According to Oliveira et al. [15], the physical vulnerability of buildings to landslides assessment is based on the following theoretical foundations: (i) the level of damage depends on the typology and magnitude of the landslide; (ii) the level of structural or non-structural damage is largely dependent on the strength of the affected element; (iii) the position of the affected element within the destabilized mass conditions the vulnerability potential; (iv) the level of damage can be qualitatively or quantitatively referenced to determine deformation patterns.

Physical vulnerability assessment methods can be grouped into two types: empirical and analytical methods. Empirical methods consist of the analysis of statistical damage from observed events, or based on expert opinion on physical vulnerability, or the assignment of a score by conducting questionnaires with different parameters to assess the potential damage of different hazardous phenomena [28]. In the case of frequent events, collecting information about the degree of physical damage to buildings or infrastructures is a quick and practical process when using damage

probability matrices or vulnerability curves. However, if there is not enough prior information regarding the damage, or if there is no funding for the application of an analytical method, the most viable option is to consult a group of experts specialized in vulnerability or in the expected damage depending on the intensity of the dangerous phenomenon [26, 28].

Analytical methods study the behavior of buildings and structures based on engineering criteria and use physical modeling tests or computer simulation techniques. In these methods, the information about the hazardous phenomenon must be more detailed, which makes these methods more demanding in terms of resources (time and money), but they allow a better understanding of the relationship between the intensity of the hazardous phenomenon and the expected degree of damage to an exposed structure. This factor ends up determining the scale when using the analytical methods since it needs a larger number and greater complexity of data, being used in the assessment of individual structures, in a smaller sample, with a large scale [26, 28].

The building's vulnerability depends on its intrinsic properties (e.g., construction material, conservation state, etc.) and the landslide's dynamic properties (type of movement, speed of movement, volume, etc.). Alves and Oliveira [2] compiled records of the physical vulnerability of different roads (rural road, municipal road; national road; and motorway) in the Grande da Pipa River basin, through a sample of 356 rainfall-triggered landslide movements; and developed an exploratory approach to assess the damage patterns to buildings and roads, resulting from these landslides. Alves [1], assessed the structural vulnerability patterns in roads and buildings generated by the impact of landslides in the same study area, to different internal sectors of the landslide mass: scarp, depletion area, accumulation area, landslide main body, and landslide front.

In this context, this work aims to assess the buildings' physical vulnerability, of the Lisbon metropolitan area (LMA), to landslides triggered by precipitation and seismic activity, individually. For this, the following objectives were defined:

(i) identify the buildings of the LMA that are in very high susceptibility areas to landslides triggered by precipitation and seismic activity;
(ii) create an index of physical vulnerability for the LMA's buildings (BGE), using the variables provided by the 2011 census data and with the support of literature;
(iii) apply the physical vulnerability index to buildings located in the most susceptible areas, either to landslides triggered by precipitation or by seismic activity.

## 2 Study Area

The LMA contains 18 municipalities (Fig. 1) and 122 parishes, in 3,015.24 $km^2$, distributed in two main areas, separated by the Tagus estuary: Greater Lisbon and the Setúbal Peninsula. At the national level, the LMA corresponds to the NUT III with the largest number of inhabitants and the second most populous, with about 2,870,770

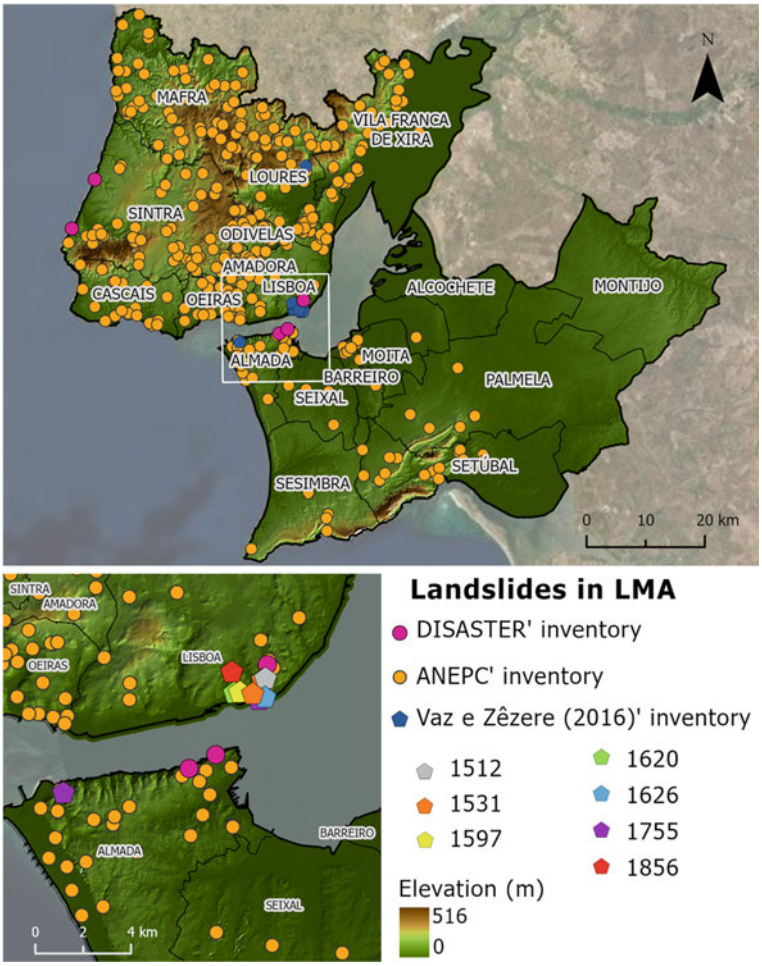


**Fig. 1** Landslide inventories triggered by rainfall and landslides in LMA

people registered in the 2021 census, which corresponds to an increase of 1.7% compared to the 2011 census, and represents about 27.8% of the total Portuguese population.

## *2.1 Geological and Geomorphological Context*

The Portuguese territory is located along the Azores-Gibraltar fault, close to the intersection of three tectonic plates, the North American Plate, the Eurasian Plate, and the African Plate [5]. Mainland Portugal is in the southwestern part of the Eurasian

Plate and constitutes an important area of seismic activity, with seismicity resulting either from phenomena derived from movements in faults at the boundaries of the plates (interplates), or from phenomena resulting from faults that are in the interior of the Eurasian plate (intraplates). Earthquakes resulting from interplate movements are typically characterized by high magnitudes and epicentral depths due to the proximity of the continental region to the boundary of the tectonic plates and to the tectonic inversion process, which began in the Quaternary, which translates into important seismic episodes, such as the 1755 earthquake [22]. While earthquakes resulting from intraplate movements have lower and more dispersed seismicity in space, with a maximum magnitude of about 6.5 on the moment magnitude scale [6]. The intersection of the Eurasian Plate with the African Plate, at the southern limit of the Iberian Peninsula, is responsible for the tension that causes the country's high seismic activity, with the converging movement of the two plates in the NNW-SSE direction, translating the subduction of the Atlantic oceanic lithosphere under the Iberian continental lithosphere [25].

Cabral [5] identified different types of faults in Portugal. In the interior and coastal regions, reverse faults predominate, with orientations NE-SW to ENE-WSW and NNE-SSW to N-S, respectively. In the north-east region of mainland Portugal, faults with unplugging movement predominate, with NNE-S orientation, and, on the western Alentejo coast, there are normal faults, namely the Grândola fault, with WNW-ESE orientation, these being the rarest faults type in Portugal. The Lower Tagus Fault is one of the main active tectonic faults in the LMA,characterized by intraplate movement, which movement was responsible for one of the most important earthquakes in the region (January 26, 1531, [31]).

LMA is divided into two morfostructural units: Meso-Cenozoic Basins and the Lower Tagus and Alvalade Cenozoic Basins [20], delimited according to the period of formation and lithological material, which results in a large and complex lithological variety and in the existence of rocks about 260 million years old [21].

On the Meso-Cenozoic Basins, there are two important regional units that are part of the AML territory: the mountains and hills between Montejunto and Lisbon and the Monoclinal Mountains of Boa Viagem and Arrábida [17]. The Mountains and Hills between Montejunto and Lisbon, with an average altitude of 173 m and an average slope of 6.9°, which main relief unit in the LMA is the Serra de Sintra, a dome with 528 m, with an east–west and with an elliptical shape, which results from the ascent of a magmatic massif, and the Lisbon Volcanic Complex, dominated by hills that are what remains of old volcanic cones, deconstructed in the current relief, which have a maximum altitude of 400 m. The Monoclinal Mountains of Boa Viagem and Arrábida present as the main unit of relief in the Arrábida mountain range, with a maximum altitude of 501 m, which stands out in the coastal platform, with a very complex monocline limestone relief, which includes subunits: the Comenda and Vale da Rasca units, the sandstones and transitional clays and the Espichel limestones, sandstones and marls; from east to west, respectively [11].

The Lower Tagus and Alvalade Cenozoic Basins include five regional relief units included in the LMA territory: the High plain of Ribatejo, with average slopes of 5.3°, with a plain situated between 60 and the 100 m, with essentially Miocene sediments,

with evidence for the Trancão river basin; the High plain of Alentejo, with an average altitude of 69 m and an average slope of 2°, characterized by the sedimentary filling surfaces; the low Tagus plain, a flat and lower area, with an average altitude of 23 m and an average slope of 1.6°, with alluvium and low sedimentary terraces of the Tagus river; the Peniche-Lisbon Coastal Plain, which corresponds to a narrow coastal sector limited by cliffs and steep slopes, with an average altitude of 70 m and an average slope of 4.6°, and with small or non-existent beaches; and the Setúbal Peninsula, with an average altitude of 43 m and an average slope of 2.3°, located between the Tagus estuary and Serra da Arrábida, whose main relief units are the Belverde platform and the fossil cliff of Costa de Caparica, a steep slope (max. altitude of 100 m) that presents slope instability and soil water erosion.

The characteristics of the varied and complex lithology of the LMA determine the spatial distribution of landslides (Fig. 1) and the way in which the terrain reacts to the passage of seismic waves. Therefore, it is crucial to pay attention to the lithology and the zoning of seismic hazards in urban occupation, in the type of construction, and in the construction of road structures [21].

## *2.2 Building Environment in the LMA*

According to 2011 census data, the LMA comprises a total of 448,957 buildings, of which 292,978 (65%) correspond to reinforced concrete buildings, 97,116 (22%) correspond to slab buildings, and 48,138 (11%) correspond to masonry buildings. There was also a small percentage of buildings, around 3%, corresponding to buildings made of adobe or loose stone masonry and other materials (7,663 and 3,062, respectively). The current building includes accommodations that were built before 1919 (22,297). The urban fabric showed an increasing evolution until 1990, and in the 30 years from 1961 to 1990, 215,799 buildings were built, which represents about 48% of current buildings.

Figure 2 illustrates the evolution of the type of building structure used in the construction of the buildings' structure over the years, corroborating the chronological scheme of Bernardo et al. [4], and proving the rise and dominance of reinforced concrete, which started in the mid-1930s. It's also significant the initial decrease and eventual disappearance of materials such as loose stone or adobe masonry walls and the masonry wall without slab from the period 1971–1980, reflecting the transition from traditional building systems and materials to current building technologies.

Moving on to the analysis of the volumetry of the buildings present in the LMA; around 69% of the buildings included in the 2011 census (309,150) correspond to buildings with 1 or 2 floors, where buildings with more than two floors representing around 31% (139,807).

Figure 3 combines the type of structural system of the building with the number of floors. Of the 309,150 buildings with 1 or 2 floors (69% of the total number of buildings), 59.7% correspond to reinforced concrete buildings, 25.2% to slab buildings, 12% to masonry buildings, and only 2.3% to buildings with loose stone


**Fig. 2** Type of building structure per date of construction periods in LMA: (1) Reinforced concrete; (2) Masonry wall with concrete elements; (3) Masonry walls without concrete elements; (4) Walls of adobe or loose stone masonry; (5) Others

or adobe masonry walls. The remaining 0.8% corresponds to buildings with 1 or 2 floors made up of other structural systems. Of the 139 807 buildings with two or more floors (31% of all LMA buildings), 77.6% have a reinforced concrete structure, 13.7% are slab buildings, 7.8% are masonry walls and only 0.4% have walls made of loose stone or adobe masonry. As in the case of buildings with 1 or 2 floors, the remaining 0.5% of buildings with two or more floors were built using other structural solutions.

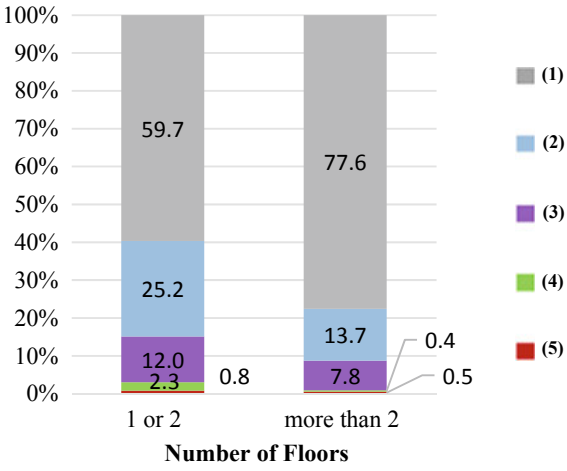


**Fig. 3** Reinforced structure and number of floors of buildings in LMA: (1) reinforced concrete; (2) slab buildings; (3) masonry buildings; (4) loose stone or adobe masonry walls; (5) other structural systems

The exterior cladding of buildings, in the LMA, has traditional plaster or marble as its predominant material, with about 93.6% of the total material, dominating during all construction periods. According to INE data from the 2011 census, 91.5% of buildings in the LMA have sloped roofs, covered with ceramic or concrete tiles.

## 3 Data and Methods

The physical vulnerability of the building located on the slip surface, for landslides triggered by rainfall and seismic activity, is evaluated at the building level, for all LMA buildings, located in very susceptible areas (9th decile) for both triggering mechanisms (Fig. 4).

### *3.1 Landslide Inventory in the LMA*

Landslide inventories were obtained in three different databases: two recorded landslides triggered by rainfall (Disaster database and the National Authority for Emergency and Civil Protection (ANEPC database) and another is a historical inventory of landslides triggered by seismic events. The location of the landslides included in each database can be found in Fig. 1.

DISASTER's national database only includes landslides that caused human damages (e.g., fatalities, injured, evacuated, displaced, and/or missing people) [36] reported in national and regional newspapers. Between 2006 and 2020, there were five damaging landslides in the LMA, where two fatalities, five injured, four displaced people, and ten affected buildings were recorded. The Disaster cases are related to damaging landslides affecting people and/or buildings. An example is the rock fall on cliffs, such as the 2018 occurrence in Colares, which resulted in one death and four injuries [39].

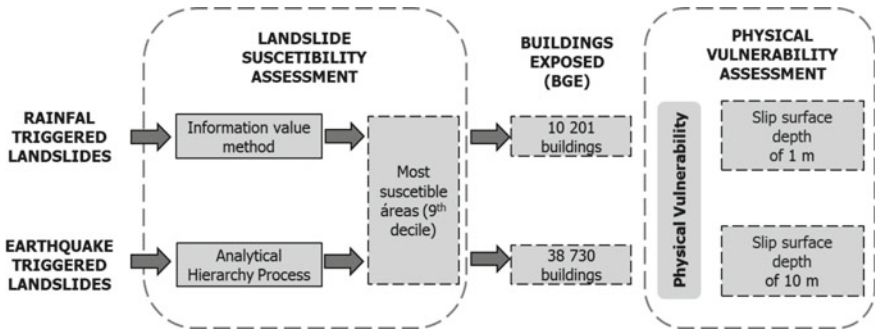


**Fig. 4** Methodological framework

The ANEPC database was cleaned in order to remove all records without description and location, reported by civil protection authorities every time there is an emergency call. Seven hundred sixty-six landslides were then identified between 2006 and 2020. The years that recorded the highest number of occurrences were 2010 (154 occurrences), 2009 (91 occurrences), 2006 (77 occurrences), 2014 (76 occurrences), and 2013 (75 occurrences), with Mafra and Loures being the most affected municipalities in these years with 165 and 123 occurrences, respectively. ANEPC database includes more numerous and dispersed landslide cases in the LMA (Fig. 1), often reporting landslides that caused obstructions on public roads and/or damages in buildings.

The inventory of historical landslides triggered by earthquakes identified by Vaz and Zêzere [30] in historical documental sources contains ten occurrences in the LMA between 1512 and 1856. The 1755 earthquake caused the largest number of landslides (3), followed by the 1531 earthquake (2). Santa Maria Maior was the most affected parish, with five landslides triggered by four different earthquakes. The landslides records triggered by earthquakes [30] cannot be dissociated from the date of occurrence, the context of the urban fabric, and the population distribution at the time of the events, since it is in places with a greater population concentration and greater urban density, that these occurrences have more visibility and impact, and therefore more documentary records are available.

### *3.2 Rainfall-Triggered Landslide Susceptibility*

Rainfall-triggered landslide susceptibility was assessed in a previous study [36] using a bivariate statistical model, the Information Value method (IV), using seven predisposing factors with 10 m cell-size (slope angle, slope exposure, slope curvature—transverse profile, geology, land use, topographic position index—TPI and topographic moisture index). Landslides were inventoried for the Lisbon and Tagus Valley region based on the interpretation of aerial photos and orthophoto maps and fieldwork in sample areas. The landslide inventory performed included 4,047 occurrences, most of them corresponding to slides (translational and rotational), which were used as a dependent variable. The information value of each class within each predisposing factor was computed to apply the IV equation, as formulated in Eq. (1) [34, 35]:

$$Ii = \ln \frac{Si/Ni}{S/N} \tag{1}$$

where l*i* is the Information Value of variable *Xi*; *Si* is the number of terrain units with landslides and the presence of variable *Xi*; *Ni* is the number of terrain units with variable X*i*; *S* is the total number of terrain units with landslides; and *N* is the total number of terrain units.

The relevance of any independent variable to discriminate between stable and unstable areas is as greater as its distance from the 0 value of IV. When the score is negative, it means that the presence of the variable X*i* is favorable to slope stability. Positive scores mean a positive relationship between the presence of the variable and the landslide occurrence, as high as the higher the score. Information values equal to zero mean no clear relationship between the variable and the landslide occurrence.

The quality of this rainfall-triggered landslide susceptibility model was assessed through the computation of ROC success rate curves and the corresponding Area Under the Curve (AUC). The rainfall-triggered landslide susceptibility was divided into five classes (very high, high, moderate, low, and very low), defined through the percentage of accumulated landslide area: 50, 70, 90, 95, and 100%, respectively. For delimiting the areas currently subject to the danger of slope instability, high and very high susceptibility classes were selected and aggregated, which together validate 70% of the landslide inventory and, which together, represent the 90th percentile of the susceptible area.

### *3.3 Earthquake-Triggered Landslide Susceptibility*

Susceptibility to landslides triggered by earthquakes was assessed with the multicriteria method of the Analytic Hierarchy Process to achieve the relative weights based on Saaty's scale of influence [23]. This technique consists of comparing predisposition factors, ranking one in relation to the other through the attribution of weights (to the variables) and scores (to the classes of variables). This technique is quite subjective as it depends on specialized knowledge of the different predisposing factors to justify the ranking of priority scales [23], in this case, this knowledge is justified with the support of bibliographic research.

There is no universal criterion for choosing predisposing factors, requiring prior technical knowledge of the hazardous phenomenon and the characteristics of the study area, and it is necessary to consider the scale of analysis and data acquisition techniques. In this model, there was used six predisposing factors (slope angle, slope curvature, TPI, geology, PGA, and distance to faults (Fig. 5)) and a historical landslide inventory (10) based on documental sources [30].

Westen et al. [32] present an overview of environmental factors and their relevance to the susceptibility of landslides and hazard assessment, considering the slope as the most important factor for gravitational movements, factors derived from the digital elevation model (DEM) (slope and profile curvature) are of high importance, as are lithology-related factors, structure-related factors, and faults [14, 32]. Slope, lithology, TPI, and curvature are also frequently used factors in susceptibility models performed for study areas located in LMA areas [8, 9].

From the DEM, with a resolution of 10 m, the slope angle, slope curvature, and TPI were generated. The lithology was obtained from the Geological Map of the Lisbon Metropolitan Area, on a 1: 25,000 scale. The five classes of distance to faults were computed with buffers of 1,000 m, 5,000 m, 10,000 m, 20,000 m, and 50,000 m,

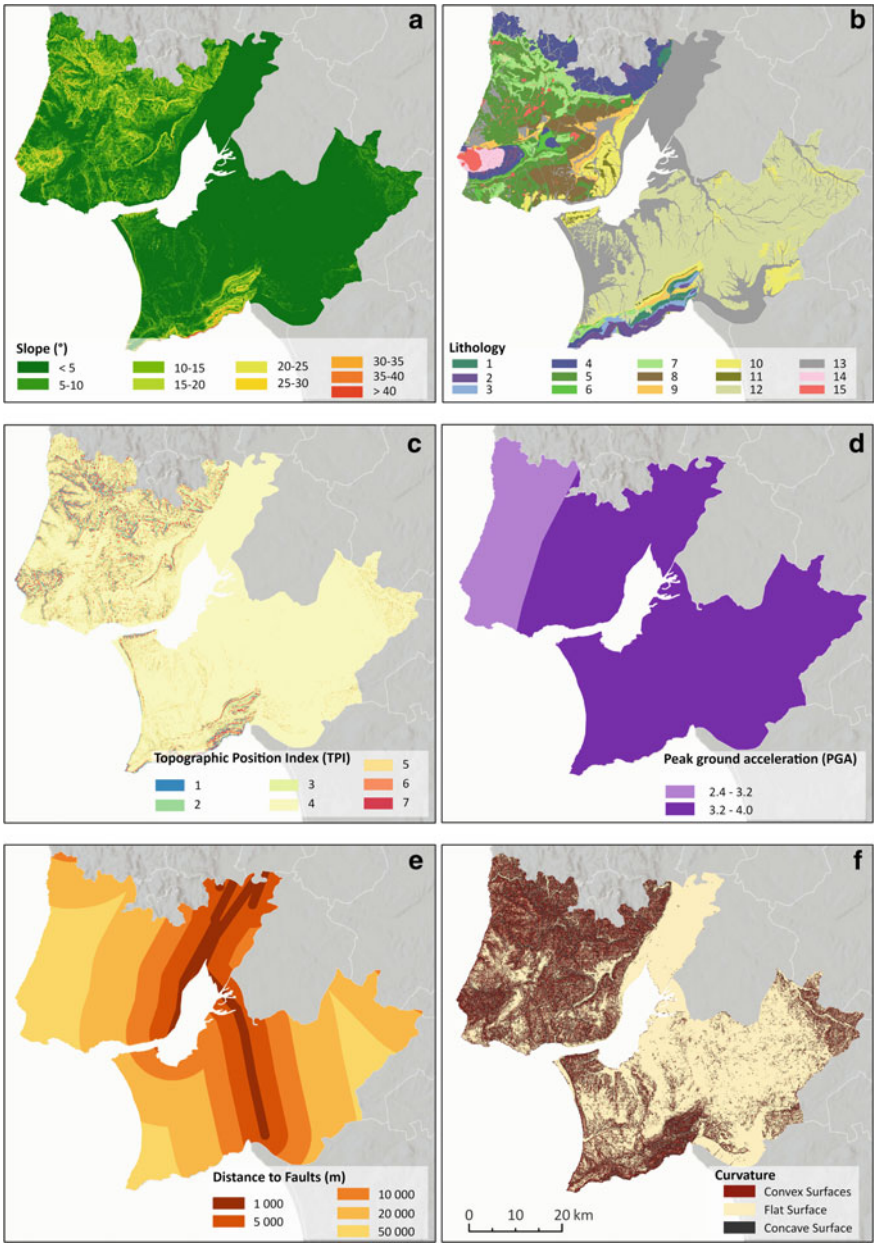


**Fig. 5** Predisposing factors and corresponding classes used to assess the earthquake-triggered landslide susceptibility. See legends in Table 2

to faults with tectonic activity provided by the Quaternary Faults Database of Iberia (QAFI). The Peak Ground Acceleration (PGA) was obtained from Peláez Montilla and López Casado [16] for a scenario of peak accelerations with a 10% probability of exceedance in 50 years (return period of 475 years).

The predisposing factors were reclassified, and the respective classes were ranked, by decreasing order of importance, where a weight was assigned to each class and a score to each class of the variable (see Table 2).

The area most susceptible to landslides triggered by earthquakes (9th decile) was selected to assess the PVB for each building exposed to landslides with a slip surface depth of 10 m. A slope movement inventory with ten occurrences [30] was used to assess the overall quality of the susceptibility model of slope movements triggered by seismic activity through the calculation of the success curve and the AUC.

### *3.4 Physical Vulnerability of Buildings*

The physical vulnerability of buildings with a residential function exposed to the most susceptible landslide was assessed for the whole LMA, using the Building Georeferencing Base (BGE) of the Portuguese Institute of Statistics (INE). This database includes 449,473 buildings for the LMA and data about the building characteristics, building type, building structure, main use, number of floors, presence of elevator, accessibility to a wheelchair, number of lodgings, period of construction, the material used in the exterior cladding of the building, type of building cover and the need for repairs (rooftop, structure, walls, and window frames).

In this work, two scenarios were considered: (i) the scenario of a given building is located in a slip surface area of 1 m, in a situation of slope instability triggered by precipitation; and (ii) the scenario of a given building is located in the 10-m slip surface area, in a situation of slope instability triggered by seismic activity. The physical vulnerability index was computed for all buildings located in high and very high susceptibility classes (90th percentile) in both scenarios (10,201 buildings in scenario (i) and 38,730 buildings in scenario (ii)).

The physical vulnerability index includes six parameters: construction material (CM), reinforced structure (RS), construction period (PC), need for repair in the structure (NRS), need for repair in the finishes (NRF), and the number of floors (NF). Each parameter was divided into a set of building classes obtained from BGE (Table 1).

Construction materials (CM) include four main types of buildings from the highest to the lowest resistance: reinforced concrete, brick or stone walls, adobe, and other materials (e.g., wood and metallic). The presence of a reinforced structure (RS) was also considered because, when present, it provides additional resistance to the building. The classes were ranked from the most to the least reinforced structure.

The construction period (CP) in the BGE database includes 11 classes, starting before 1919 until 2011. The construction period indirectly indicates the conservation status and the construction quality of buildings per historical period. This variable was

**Table 1** Vulnerability index formulation: parameters, classes and respective weights

| Parameters and classes | | RTL | ETL |
|---|---|---|---|
| | | Slip surface depth 1 m | Slip surface depth 10 m |
| CM | Reinforced concrete | 0.3 | 0.91 |
| | Brick and stone | 0.43 | 0.99 |
| | Adobe | 0.59 | 1.00 |
| | Other (Wood, metallic, etc.) | 0.64 | 1.00 |
| RS | Reinforced concrete | 0.3 | 0.91 |
| | Masonry walls with concrete elements | 0.3 | 0.91 |
| | Masonry walls. without concrete elements | 0.43 | 0.99 |
| | Walls of adobe or loose stone masonry | 0.59 | 1.00 |
| | Other (Wood, metallic, etc.) | 0.64 | 1.00 |
| CP | >1991 | 0.3 | 0.3 |
| | 1961 < 1991 | 0.5 | 0.5 |
| | 1919 < 1961 | 0.7 | 0.7 |
| | <1919 | 0.9 | 0.9 |
| NRS and NRF | Does not require repairs | 0.2 | 0.2 |
| | Requires minor repairs | 0.4 | 0.4 |
| | Requires medium repairs | 0.6 | 0.6 |
| | Requires large repairs | 0.8 | 0.8 |
| | Requires major repairs | 1 | 1 |
| NF | >2 | 0.3 | 0.3 |
| | 1 or 2 | 0.5 | 0.5 |

divided into four classes from the lowest to the highest building feature class weight: (i) the period before 1919 to include the most ancient and historical buildings, with adobe/rubble masonry and the unreinforced masonry buildings with timber floor; (ii) the period between 1919 and 1960 to include the two World Wars periods and the shortage of construction materials, such as steel. At this time, there was the emergence of the "Placa" buildings, in Lisbon, constructed with regular geometry; (iii) the period between 1960 and 1990, characterized by the use of better construction techniques, including the use of concrete; and (iv) the period after 1990, when the buildings have a good quality with reinforced construction materials [12, 33].

The need for repair in the structure (NRS) and in the finishes (NRF) includes five classes: "does not require repairs," "requires minor repairs," "requires medium repairs," "requires large repairs," and "requires major repairs."

**Table 2** AHP scores for each predisposing factor class to assess earthquake-triggered landslide susceptibility

| | ID | Class | Class score | Variable weight |
|---|---|---|---|---|
| Slope angle | 1 | <5 | 0.019 | 0.460 |
| | 2 | 5–10 | 0.026 | |
| | 3 | 10–15 | 0.037 | |
| | 4 | 15–20 | 0.053 | |
| | 5 | 20–25 | 0.076 | |
| | 6 | 25–30 | 0.109 | |
| | 7 | 30–35 | 0.154 | |
| | 8 | 35–40 | 0.218 | |
| | 9 | >40 | 0.307 | |
| Lithology | 1 | Sandstones–Cretaceous | 0.045 | 0.256 |
| | 2 | Sandstones–Jurassic | 0.164 | |
| | 3 | Limestones–Cretaceous | 0.264 | |
| | 4 | Limestones–Jurassic | 0.264 | |
| | 5 | The volcanic complex of Lisbon | 0.1 | |
| | 6 | Volcano-sedimentary complex | 0.068 | |
| | 7 | Quaternary deposits | 0.068 | |
| | 8 | Granite | 0.024 | |
| | 9 | Marls and limestones | 0.335 | |
| | 10 | Marls and limestones–Jurassic | 0.335 | |
| | 11 | Other rocks–Miocene | 0.045 | |
| | 12 | Other acid magmatic rocks | 0.045 | |
| | 13 | Clayey rocks–Miocene | 0.068 | |
| | 14 | Detrital rocks–Paleogene | 0.164 | |
| | 15 | Detrital rocks–Pliocene | 0.045 | |
| TPI | 1 | V-shaped valleys | 0.114 | 0.114 |
| | 2 | Moderate fit valleys. half slope drainage | 0.114 | |
| | 3 | U-shaped valleys | 0.114 | |
| | 4 | Flat areas and slope toe | 0.045 | |
| | 4 | Flat areas and slope base | 0,045 | |
| | 5 | Middle Slope | 0.317 | |
| | 6 | Upper Slope | 0.524 | |
| | 7 | Top slope | 0.045 | |
| PGA | 1 | 3.2–4.0 | 0.539 | 0.087 |
| | 2 | 2.4–3.2 | 0.297 | |

(continued)

**Table 2** (continued)

| | ID | Class | Class score | Variable weight |
|---|---|---|---|---|
| Distance to faults | 1 | 1 000 | 0.462 | 0.051 |
| | 2 | 5 000 | 0.256 | |
| | 3 | 10 000 | 0.142 | |
| | 4 | 20 000 | 0.088 | |
| | 5 | 50 000 | 0.052 | |
| Slope curvature | 1 | Convex | 0.257 | 0.032 |
| | 2 | Rectilinear | 0.074 | |
| | 3 | Concave | 0.669 | |

The number of floors (NF) is a proxy variable of the foundations' depth, because the higher the building, the deeper and more resistant the foundations should be Silva and Pereira [26]. In this work, two classes of the number of floors were considered: 1 or 2 floors and more than two floors.

A score was given to each building class and the respective parameter (see Table 1) for both triggering scenarios. Both scores and parameters' weights are based on expert opinion and dedicated literature (Table 1). For instance, construction material and reinforced structure were obtained from Guillard-Goncalves et al. [10], where an average vulnerability value was assigned to a study area located in Loures municipality. The scores obtained by Guillard-Goncalves et al. [10] were based on a questionnaire applied to a pool of 14 experts with field-based knowledge of landslides in the area north of Lisbon.

The weights assigned to each parameter of the physical vulnerability index (PVI) were based on a previously published work [18] applied to the municipality scale in Portugal, where the material construction has more importance, followed by the reinforced structure and number of floors. Because this index presents two more variables than Pereira et al. [18], it was necessary to adapt the weights, including the need for repairs to the structure and the need for repairs to the structure (NRS and NRF), which have the same weight as the construction period (PC) (0.1). The PVI was weighted according to Eq. (2):

$$PVI = 0.3CM + 0.2(RS + NF) + 0.1(PC + NRS + NRF) \quad (2)$$

Then, a cluster analysis was performed through the "Multivariate Clustering" tool available in ArcGIS Pro software, using the k means method to divide the buildings into four different groups, depending on the PVI parameters.

# 4 Results

## *4.1 Landslide Susceptibility and Exposure*

Table 2 presents the predisposition factors and their weights, with the respective classes of each predisposition factor and each score, and Fig. 5 presents the spatial distribution of each predisposing factor.

Slope angle comprehends nine classes: <5; 5–10; 10–15; 15–20; 20–25; 25–30; 30–35; 35–40; >40, where classes with a higher slope angle present a higher score. Lithology has 15 classes: Volcano-sedimentary complex; Limestones (Jurassic); Sandstones (Jurassic); Marls and limestones (Jurassic); Limestones (Cretaceous); Marls and limestones; Sandstones (Cretaceous); 8—Volcanic complex of Lisbon; Detrital rocks (Paleogene); Other rocks (Miocene); Clayey rocks (Miocene); Detrital rocks (Pliocene); Quaternary deposits; Granite; Other acid magmatic rocks. TPI classes include V-shaped valleys; Moderate fit valleys, half slope drainage; U-shaped valleys; Flat areas, and slope base; Middle slope; Upper slope; and Top slope. In LMA, there are two classes of PGA, 2.4–3.2 and 3.2–4.0. Distance to faults' buffers is divided into five classes, with scores deriving according to the proximity. Slope curvature has three classes—convex, rectilinear, and concave—with a higher score for the concave areas, where a greater deposition of soil occurs.

The variable weights achieved by the Analytic Hierarchy Process, based on Saaty's scale of influence [23], were: slope, with a weight of 0.460,lithology, with a weight of 0.256; TPI, with a weight of 0.114; PGA, with a weight of 0.087; distance to faults, with a weight of 0.051; and curvature, with a weight of 0.032. Since the AHP susceptibility model obtained a consistency index of 0.06 and a consistency ratio of 0.05, which are <0.1, we can assume that our metric is reasonably consistent in the process of decision-making.

The quality of the susceptibility models was assessed through the computation of the ROC success curve and the AUC. The success curve consists of the comparison between the image of the susceptibility model and the identified slope movements used in the model. Figure 6 shows the ROC success rate curve of the rainfall-triggered landslide (RTL)) susceptibility model and the earthquake-triggered landslide (ETL) susceptibility model, according to the proportion of area correctly classified as susceptible (TPR) and the proportion of non-landslide area classified as susceptible (FPR). The ETL model hits with high quality the proportion of identified landslide inventory, with an AUC = 0.93, while the ETL model has a very satisfactory quality with an AUC of 0.82.

Figure 7 presents (A) the susceptibility map for landslides triggered by precipitation; and (B) the susceptibility map for landslides triggered by seismic events. The susceptibility is represented in 5 classes divided into quintiles—Very Low, Low, Moderate, High, and Very High.

Both landslide susceptibility models were used to filter buildings located in the most susceptible areas (90th percentile) to RTL and ETL (see Figs. 8s and 9a, respectively). Of the total number of buildings in the LMA (449,473), there are 10,201

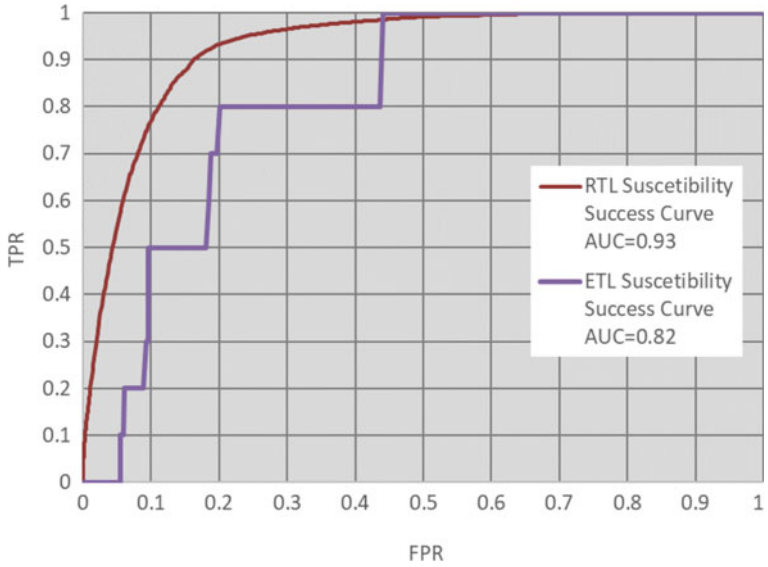


**Fig. 6** ROC success rate curves of RTL and ETL susceptibility models

buildings in the areas most susceptible to RTL and 38,730 buildings in the areas most susceptible to ETL.

## *4.2 Physical Vulnerability of Buildings*

Figure 8a shows the physical vulnerability of buildings (PVB) exposed to the 90th percentile of susceptibility to RTL, and Fig. 8b represents the average physical vulnerability per parish for a slip surface area of 1 m. Physical vulnerability is represented by five classes (Very Low, Low, Moderate, High, and Very High), divided into quintiles. The municipalities of Lisbon and Loures present the buildings with the highest physical vulnerability index in the case of RTL. Cascais, Oeiras, and Odivelas municipalities present the lowest average vulnerability values per parish.

Figure 9a shows the physical vulnerability of buildings exposed to the 90th percentile of susceptibility to ETL and Fig. 9b represents the average physical vulnerability per parish for a slip surface area of 10 m. Physical vulnerability is represented by five classes divided into quintiles. The municipalities of Lisbon present the buildings with the highest physical vulnerability index in the case of ETL. Cascais and Oeiras municipalities present the lowest average vulnerability values per parish.

The physical vulnerability to RTL ranges from 0.28 (minimum value and 1st quartile) to 0.71 (maximum value), records and an average value of 0.34 and the median corresponds to 0.32. The physical vulnerability index for ETL ranges between 0.585 and 0.89, records an average value of 0.65 and the median is 0.645. The PVB

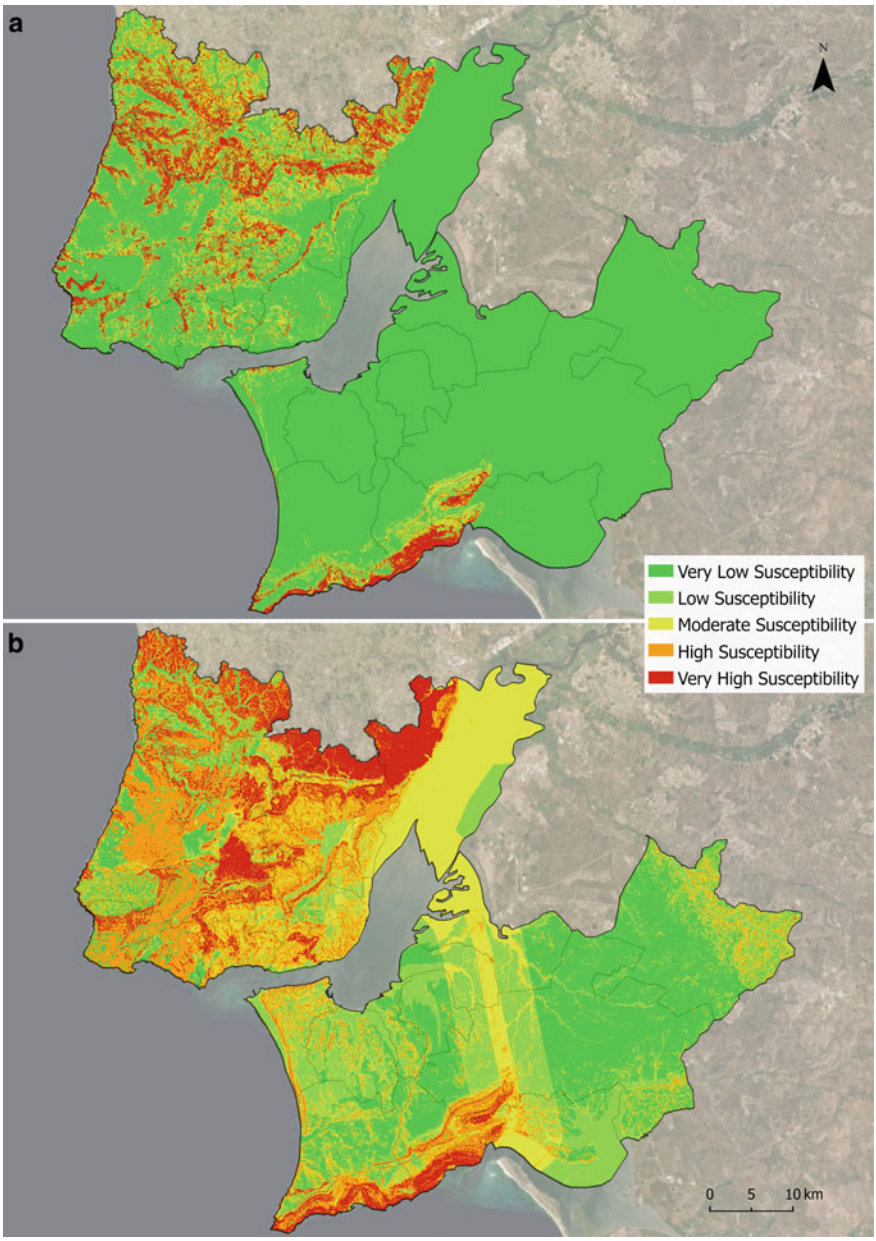


**Fig. 7** **a** RTL susceptibility and **b** ETL susceptibility in the LMA

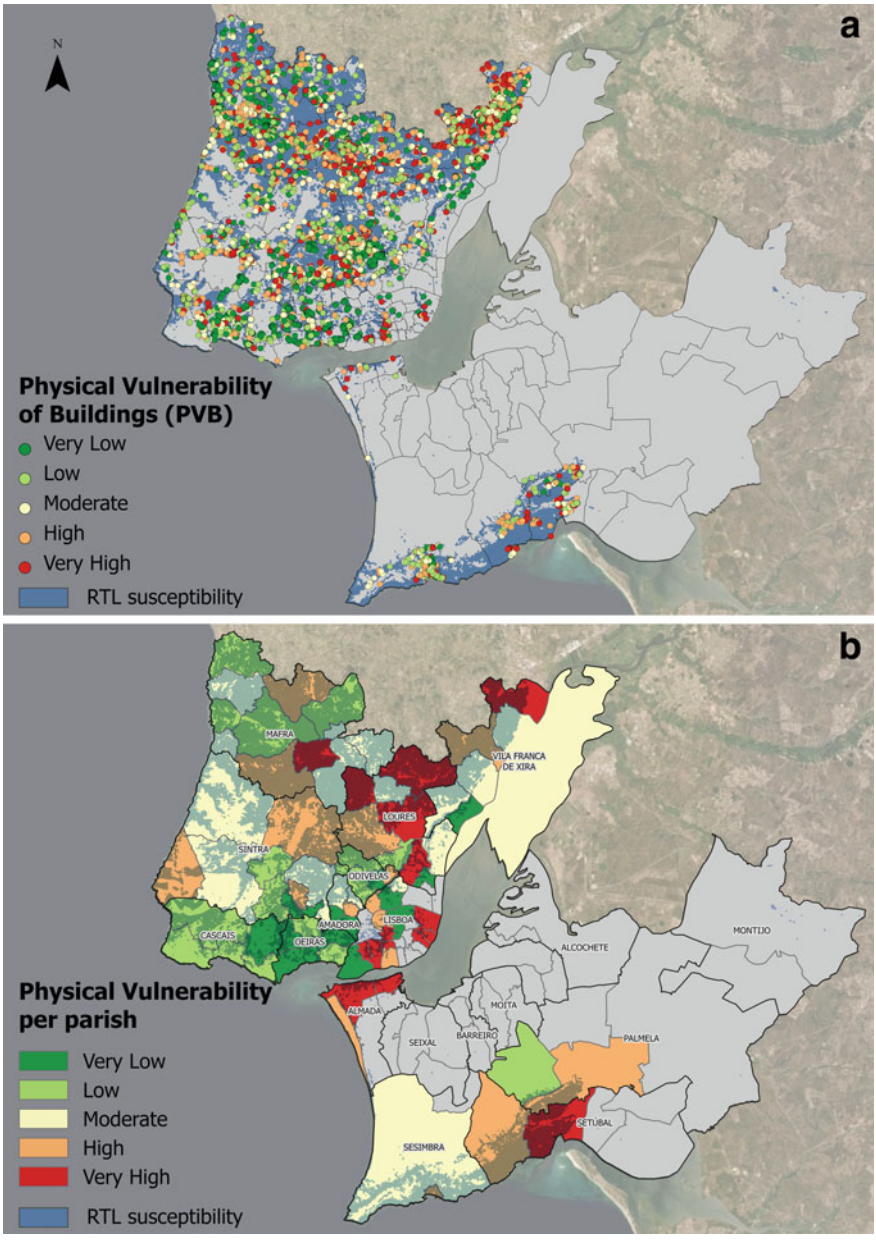


**Fig. 8** Physical vulnerability of buildings (**a**) and the average physical vulnerability scores per parish (**b**) of buildings located in the 90th percentile of RTL susceptibility in the LMA (1 m slip surface scenario)

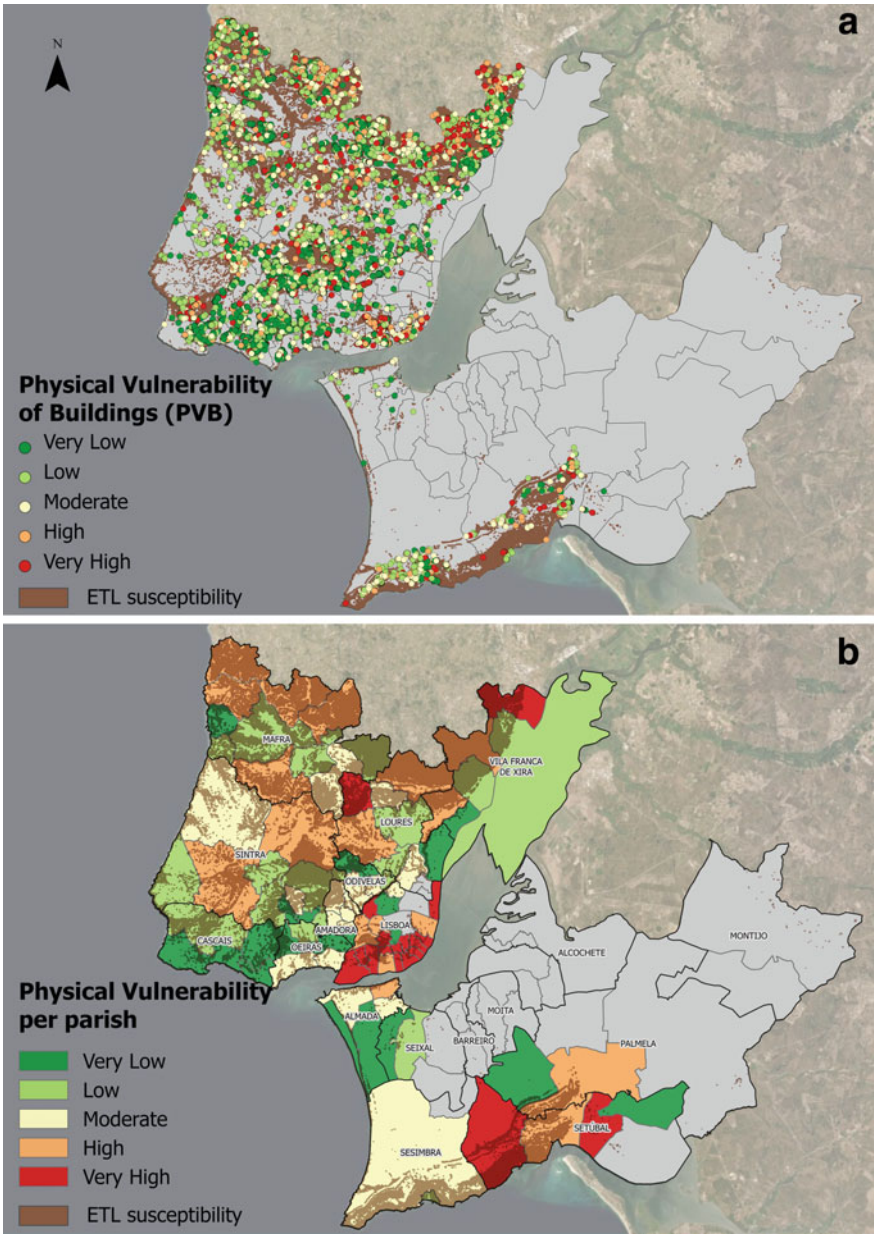


**Fig. 9** Physical vulnerability of buildings (**a**) and the average physical vulnerability scores per parish (**b**) of buildings located in the 90th percentile of ETL susceptibility in the LMA (10 m slip surface scenario)

for RTL presents lower values than for ETL, which reflects the difference in the scores attributed to the classes of variables corresponding to the construction material and the reinforced structure, for both scenarios.

Figure 10 presents a spatial distribution of the cluster analysis, performed with the physical vulnerability of buildings exposed to the most susceptible areas of RTL (Fig. 10a) and ETL (Fig. 10b). In both landslide triggering scenarios, 4 clusters were identified. Figure 11 shows the physical vulnerability parameters standardized values for each cluster in the most susceptible areas to RTL (a) and ETL (b).

In the PVB located in the most susceptible areas of RTL (Fig. 10a), Group 1 has 2,760 buildings, group 2 has 1,397 buildings, group 3 has only 295 buildings, and group 4 has the highest number of buildings (5,749). Buildings belonging to Cluster 1 recorded an average PVI of 0.35, a number of floors of 0.5, and a period of construction of 0.43, while the other parameters recorded an average PVI below 0.35 (Fig. 11a). Cluster 1 is characterized by the presence of buildings one floor, constructed between 1961 and 1990 and after 1991, with more resistant structures and construction material and in a good state of maintenance.

Cluster 4 has the lowest PVI mean value (0.3) and period of construction (0.38), and the other parameters are below 0.35. This means that buildings included in Cluster 4 are mainly constructed with two or more floors, more recently, after 1991, with more resistant structures and construction material and in a good state of maintenance.

Cluster 2 recorded a mean PVI of 0.45, period of construction (0.65), with need to repairs ($\geq$0.6), and construction material and reinforced structure with a mean PVI below 0.4. This cluster includes more ancient buildings, with slab or masonry walls, with less resistant structures and need for repairs.

Cluster 3 presents the highest mean PVI (0.55), construction material and reinforced structure (0.6), and period of construction (0.65). The buildings included in this cluster are more vulnerable because they were built with less resistant structures and materials in a period before 1919 and between 1919–1945. Buildings belonging to cluster 3 can be found mostly in Loures, Mafra, and Vila Franca de Xira' parishes.

In the PVB located in the most susceptible areas of ETL (Fig. 10b), Group 1 has 20,239 buildings, this being the most representative group; group 2 has 4,477 buildings; group 3 has the fewest buildings (3,812); and group 4 contains 10,202 buildings. Cluster 1 recorded the lowest mean PVI (0.6), period of construction (0.45), and number of floors (0.3). We can find more resistant buildings in this cluster, with a higher number of floors, constructed more recently (between 1961 and 1990 and after 1991).

Cluster 4 has slightly higher mean values when compared with cluster 1, but it records a higher PVI associated with the number of floors (1 or 2 floors).

Clusters 2 and 3 are very similar in all building parameters, except for the need for repairs, which has higher PVI mean values in cluster 2. In cluster 2, it is also possible to observe the highest mean PVI of all clusters. Buildings belonging to cluster 2 can be found mostly in Lisbon, Sintra, and Vila Franca de Xira parishes.

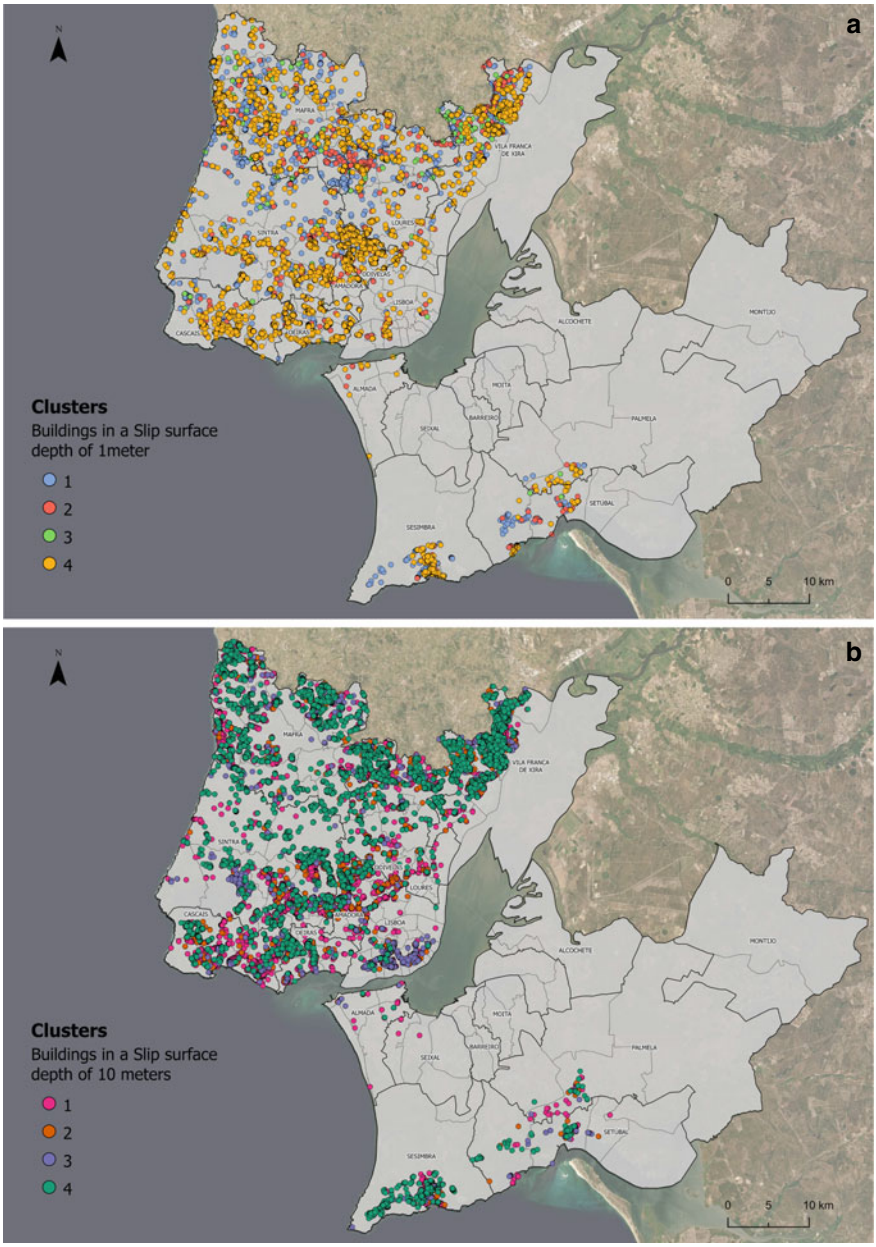


**Fig. 10** Clusters of PVB located in the most susceptible areas to RTL (**a**) and ETL (**b**) scenarios

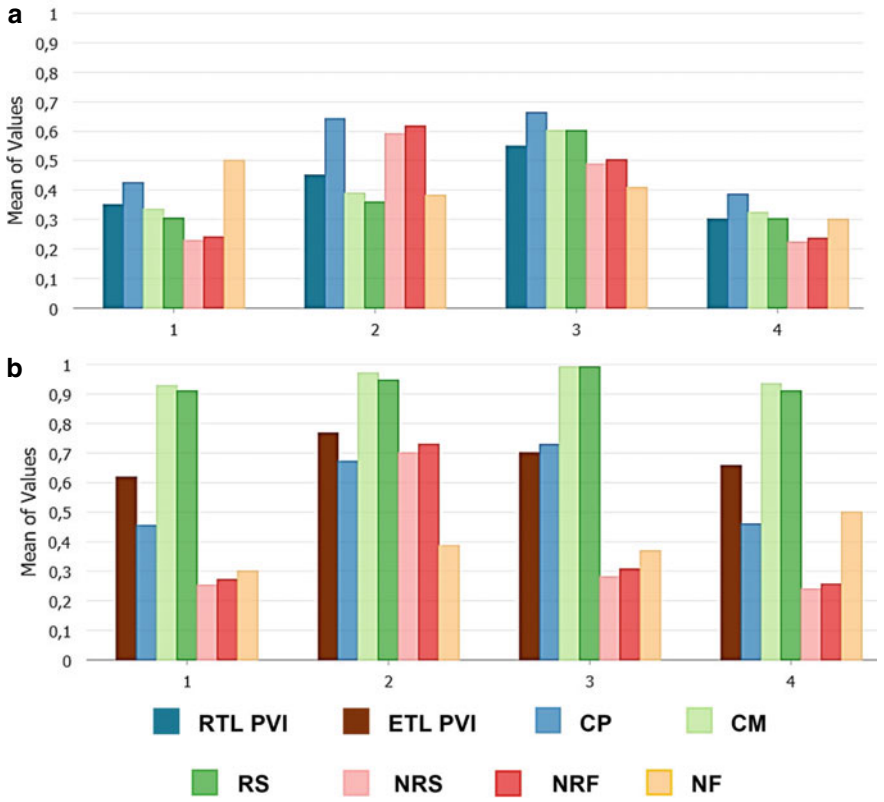


**Fig. 11** Physical vulnerability parameters and corresponding mean values of PVI for each cluster in the most susceptible areas to RTL (**a**) and ETL (**b**) scenarios

## 5 Final Remarks

In this work, the buildings exposed to two landslide triggering scenarios were identified, and an indicator-based model of the PVB was carried out to find the buildings most vulnerable to this natural phenomenon. The two scenarios correspond to the analysis of the 10 201 buildings exposed to a very high susceptibility to landslides triggered by rainfall (RTL) (Fig. 8); and the analysis of the 38,730 buildings exposed to a very high susceptibility to slope movements triggered by seismic events (Fig. 9).

A landslide susceptibility model was produced for each triggering scenario, although it is necessary to highlight the limitations associated with each susceptibility model validation. The RTL susceptibility model was validated through photo-interpretation inventories (4,047 landslides) and some field validation. The ETL susceptibility model, on the other hand, was validated through a rather small historical inventory (10 landslides). The location of the buildings was not very accurate, as well.

In this way, it would be important in the future to attest to the quality of models with more recent events. The susceptibility to ETL was modeled through the Analytic Hierarchy Process (multicriteria analysis method), which implies a subjective hierarchy, based on expert opinion and previous studies; lacking a ground validation of the quality of susceptibility and a validation of the model through occurrences of landslides triggered by future seismic events.

The very high susceptible areas to RTL are more restricted to the most hazardous slopes in the LMA (339.54 $km^2$) located in the hills in the north of Lisbon and in the Arrábida chain, and the very high susceptible areas to ETL (309.91 $km^2$) are around the same main locations but with larger features. This is the first time that these approaches have been evaluated jointly for the entire LMA.

The analysis of buildings exposed to slope movements in a scenario where the building is located in the slip surface area, for the two scenarios, was only carried out for areas with very high susceptibility; this is limiting the analysis to the 90th percentile of susceptibility. This does not mean that there cannot be damage to buildings belonging to areas with high susceptibility, for example, areas with an 80th percentile of susceptibility; however, in this work, it was assumed that we only worked with 10% of the most susceptible areas in the entire LMA, for both scenarios (RTL and ETL). Sliding failure of foundations, depth of the landslide, and impact direction affect the building damage. For instance, longitudinal impact leads to a larger contact area and a small resistance moment, which can generate severe damage to the buildings, although these scenarios were not considered. Future studies should consider a wide range of worst scenarios in landslide-building interaction studies.

The physical vulnerability index (PVI) was based on bibliographic support [10, 18]. Uncertainties can be quantified from the input parameters to the vulnerability estimates and the weights are often based on expert judgment, which seems subjective. However, for the LMA, there is not a good inventory of damages generated by landslides and the characteristics of the respective buildings affected. This makes it difficult to legitimize the scores and weights assigned to classes and variables, respectively and to apply a quantitative vulnerability model developed by statistical analysis or post-events data.

The variables used to perform the physical vulnerability index (PVI) were taken from the Building Georeferencing Base (BGE) of the 2011 census date. This information is out of date since there is already a 2021 census; however, information and data about the characteristics of the buildings were not made available at the time of this work, and there may be missing information regarding new buildings built in the last ten years.

In the LMA, it was found that the most problematic PVB areas, for both scenarios (RTL and ETL), correspond to the parish of Lisbon, presenting an average of buildings with higher physical vulnerability. There is a big difference in the variation of the PVB index values for a slip surface area of 1 m for an RTL (ranges between 0.28 and 0.71), and for a slip surface area of 10 m for an ETL (ranges between 0.585 and 0.89). This reflects the different scores attributed to the variables of construction material and reinforced structure in the two scenarios [10, 18], which correspond to the variables with greater weight in the PVI.

This study is carried out on a building scale for the entire territory of LMA, i.e., a large study area with a small scale. However, this work presents a lot of potential for analysis and future complements; for example, in a larger scale study, at the level of street/block analysis, through the identification of multi-risk hotspot areas and the identification of safe or evacuation areas for the resident population. Through the hotspots, it would be possible to identify priority risk prevention areas and implement local strategies to reduce the physical vulnerability of buildings and their exposure to landslides triggered by future rainfall and earthquake events, with detailed studies and detailed technical protection interventions (on-site intervention). This more in-depth study can also be carried out at the level of the municipality (making the hierarchy of parishes according to the average value of PVI) and at the level of the parish.

**Acknowledgements** The project 'MIT-RSC—Multi-risk Interactions Towards Resilient and Sustainable Cities' (MIT-EXPL/CS/0018/2019) leading to this work is co-financed by the ERDF—European Regional Development Fund through the Operational Program for Competitiveness and Internationalisation—COMPETE 2020, the North Portugal Regional Operational Program—NORTE 2020 and by the Portuguese Foundation for Science and Technology—GCT under the MIT Portugal Program at the 2019 PT call for Exploratory Proposals in 'Sustainable Cities'. Pedro P. Santos is financed through FCT I.P., under the contract CEECIND/00268/2017.

## References

1. Alves C (2018) Padrões de vulnerabilidade estrutural em estradas e edifícios associados à ocorrência de movimentos de vertente [Dissertação de Mestrado]. Instituto de Geografia e Ordenamento do Território
2. Alves C, Oliveira S (2017) Vulnerabilidade física das estradas a deslizamentos. In: Gomes A, Teixeira S, Soares L (eds) Atas do VIII Congresso Nacional de Geomorfologia. Associação Portuguesa de Geomorfólogos, pp 63–66
3. Araújo JR, Ramos AM, Soares PMM, Melo R, Oliveira SC, Trigo RM (2022) Impact of extreme rainfall events on landslide activity in Portugal under climate change scenarios. Landslides. https://doi.org/10.1007/s10346-022-01895-7
4. Bernardo V, Sousa R, Candeias P, Costa A, Campos Costa A (2021) Historic appraisal review and geometric characterization of old masonry buildings in lisbon for seismic risk assessment. Int J Archit Herit, 1–21. https://doi.org/10.1080/15583058.2021.1918287
5. Cabral J (1995) Neotectónica em Portugal continental. Memórias Dos Serviços Geológicos de Portugal, 31
6. Cabral J, Moniz C, Ribeiro P, Terrinha P, Matias L (2003) Analysis of seismic reflection data as a tool for the seismotectonic assessment of a low activity intraplate basin—the Lower Tagus Valley (Portugal). J Seismolog 7(4):431–447. https://doi.org/10.1023/B:JOSE.0000005722.23106.8d
7. Daveau S (2004) A Estremadura. In: Feio M, Daveau S (eds) O relevo de Portugal: grandes unidades regionais, vol 2, pp 61–74. Associação Portuguesa de Geomorfólogos
8. Gordo C, Zêzere JL, Marques R (2019) Landslide susceptibility assessment at the basin scale for rainfall- and earthquake-triggered shallow slides. Geosciences 9(6). https://doi.org/10.3390/geosciences9060268
9. Guillard C, Zezere J (2012) Landslide susceptibility assessment and validation in the framework of municipal planning in Portugal: the case of Loures municipality. Environ Manage 50(4):721–735. https://doi.org/10.1007/s00267-012-9921-7

10. Guillard-Goncalves C, Zêzere JL, Pereira S, Garcia RAC (2016) Assessment of physical vulnerability of buildings and analysis of landslide risk at the municipal scale: application to the Loures municipality, Portugal. Nat Hazard 16(2):311–331. https://doi.org/10.5194/NHESS-16-311-2016
11. Kullberg JC, Rocha RB, Soares AF, Rey J, Terrinha P, Azerêdo AC, Callapez P, Duarte LV, Kullberg MC, Martins L, Miranda R, Alves C, Mata J, Madeira J, Mateus O, Moreira M, Nogueira CR (2013) A Bacia Lusitaniana: Estratigrafia, Paleogeografia e Tectónica. In: Dias R, Araújo A, Terrinha P, Kullberg JC (eds) Geologia de Portugal, vol II, 1st ed. Escolar Editora, pp 195–350
12. Malheiros J, Zêzere J, Ludovici A, Pereira S, Oliveira S, Malheiros M (2018) Um século de respostas habitacionais públicas a catástrofes—Experiências passadas e reflexões para o future, pp 365–405
13. Martins A (2004) As bacias sedimentares do Baixo Tejo e do Sado. In: Feio M, Daveau S (eds) O relevo de Portugal: grandes unidades regionais, vol 2, pp 49–60. Associação Portuguesa de Geomorfólogos
14. Oliveira S (2012) Incidência espacial e temporal da instabilidade geomorfológica na bacia do Rio Grande da Pipa (Arruda dos Vinhos) [Dissertação de Doutoramento]. Instiuto de Geografia e Oedenamento do Território
15. Oliveira S, Zêzere JL, Garcia RAC, Pereira S (2016) Padrão de deformação de movimentos de vertente em áreas periurbanas associados a eventos de instabilidade. In: International conference on urban risks: Atas ICUR2016, pp 363–370
16. Peláez Montilla JA, López Casado C (2002) Seismic hazard estimate at the Iberian Peninsula. Pure Appl Geophys 159(11):2699–2713. https://doi.org/10.1007/s00024-002-8754-3
17. Pereira DI, Pereira PJS, Santos LJC, Silva JM (2014) Unidades Geomorfológicas de Portugal Continental. Revista Brasileira de Geomorfologia 15(4):567–584. https://doi.org/10.20502/rbg.v15i4.549
18. Pereira S, Santos PP, Zêzere JL, Tavares AO, Garcia RAC, Oliveira SC (2020) A landslide risk index for municipal land use planning in Portugal. Sci Total Environ 735:139463. https://doi.org/10.1016/j.scitotenv.2020.139463
19. Pina C, Alvarenga M, Pereira L (2019) O Ordenamento do Território na Resposta às Alterações Climáticas Contributo para os PDM
20. Ramos C, Ramos-Pereira A (2020) Landscapes of Portugal: paleogeographic evolution, tectonics and geomorphology. In Vieira G, Zêzere JL, Mora C (eds) Landscapes and landforms of Portugal. Springer International Publishing, pp 3–31. https://doi.org/10.1007/978-3-319-03641-0_1
21. Ramos-Pereira A (2003) Geografia Física e Ambiente—Diversidade do Meio Físico e Recursos Naturais. Atlas Da Área Metropolitana de Lisboa. Área Metropolitana de Lisboa, Lisboa, pp 47–65
22. Roque A (2007) Tectonostratigrafia do Cenozóico das margens continentais Sul e Sudoeste portuguesas: um modelo de correlação sismostratigráfica [Tese de doutoramento, Universidade de Lisboa]. http://hdl.handle.net/10451/1521
23. Saaty T (2008) Decision making with the analytic hierarchy process. Int J Serv Sci 1:83–98. https://doi.org/10.1504/IJSSCI.2008.017590
24. Santos M, Fonseca A, Fragoso M, Santos JA (2019) Evolução recente e futura de índices de extremos de precipitação em Portugal continental. In: Pereira A, Leal M, Bergonse R, Trindade J, Reis E (eds) Água e Território: um tributo a Catarina Ramos, Issue July. Universidade de Lisboa, Centro de Estudos Geográficos, pp 279–294. https://doi.org/10.33787/CEG20190005
25. Senos ML, Carrilho F (2003) Sismicidade de Portugal continental. Física de La Tierra 15:93–110
26. Silva M, Pereira S (2014) Assessment of physical vulnerability and potential losses of buildings due to shallow slides. Nat Hazards 72(2):1029–1050. https://doi.org/10.1007/s11069-014-1052-4
27. Sterlacchini S, Akbas S, Blahůt J, Mavrouli O, Garcia C, Quan Luna B, Corominas J (2014) Methods for the characterization of the vulnerability of elements at risk. In: Advances in natural

and technological hazards research, vol 34, pp 233–273. https://doi.org/10.1007/978-94-007-6769-0_8
28. van Westen C, Kingma N (2011) Session 5: vulnerability assessment. In: van Westen CJ, Alkema D, Damen MCJ, Kerle N, Kingma NC (eds) Multi-hazard risk assessment: distance education course/Guide book. United Nations University–ITC School on Disaster Geoinformation Management, pp 5; 1–5; 33
29. Vaz T (2010) Contribuição para o estudo dos movimentos de vertente desencadeados por eventos sísmicos em Portugal Continental [Msc Dissertation, Universidade de Lisboa]. https://repositorio.ul.pt/handle/10451/3873
30. Vaz T, Zêzere JL (2016) Landslides and other geomorphologic and hydrologic effects induced by earthquakes in Portugal. Nat Haz 81(1):71–98. https://doi.org/10.1007/S11069-015-2071-5/FIGURES/11
31. Vaz T, Zêzere JL (2020) The urban geomorphological landscape of Lisbon. In: Vieira G, Zêzere JL, Mora C (eds) Landscapes and landforms of Portugal. World geomorphological landscapes. Springer, p. 295–303. https://doi.org/10.1007/978-3-319-03641-0_23
32. Westen CJ, Castellanos E, Kuriakose S (2008) Spatial data for landslide susceptibility, hazard, and vulnerability assessment: an overview. Eng Geol 102:112–131. https://doi.org/10.1016/j.enggeo.2008.03.010
33. Xofi M (2021) Evaluation of exposure and vulnerability indicators for assessing multi-hazard risk in urban areas. Am J Orthod Dentofac Orthop, no 2. https://doi.org/10.1016/j.ajodo.2021.06.008
34. Yin KL, Yan TZ (1988) Statistical prediction models for instability of metamorphosed rocks. Int Symp Lands 5:1269–1272
35. Zêzere JL (2002) Landslide susceptibility assessment considering landslide typology. A case study in the area north of Lisbon (Portugal). Nat Haz Earth Syst Sci 2(1–2):73–82. https://doi.org/10.5194/NHESS-2-73-2002
36. Zêzere JL (2020) Geomorphological hazards. In: Vieira G, Zêzere JL, Mora C (eds) Landscapes and landforms of Portugal. Springer International Publishing, pp 47–62. https://doi.org/10.1007/978-3-319-03641-0_3
37. Zêzere JL, Pereira S, Tavares AO, Bateira C, Trigo RM, Quaresma I, Santos PP, Santos M, Verde J (2014) DISASTER: a GIS database on hydro-geomorphologic disasters in Portugal. Nat Haz 72(2):503–532. https://doi.org/10.1007/S11069-013-1018-Y
38. Zêzere JL, Trigo RM, Fragoso M, Oliveira SC, Garcia RAC (2008) Rainfall-triggered landslides in the Lisbon region over 2006 and relationships with the North Atlantic oscillation. Nat Haz Earth Syst Sci 8(3):483–499. https://doi.org/10.5194/NHESS-8-483-2008
39. Sintra Notícias. (2018 March 15) Morreu uma das vítimas na derrocada de fa-lésia na praia da Ursa. Sintra Notícias. https://sintranoticias.pt/2018/03/15/ultima-hora-derrocada-falesia-na-praia-da-ursa-sintra/